

# A first principles simulation study of vibrational spectral diffusion in aqueous NaBr solutions: Dynamics of water in ion hydration shells

Anwesa Karmakar, Jyoti Roy Choudhuri, Vivek K. Yadav, Bhabani S. Mallik<sup>1</sup>, Amalendu Chandra<sup>\*</sup>

Department of Chemistry, Indian Institute of Technology Kanpur, Kanpur 208016, India

## ARTICLE INFO

### Article history:

Received 19 September 2012

In final form 14 November 2012

Available online 7 December 2012

### Keywords:

Hydration of bromide ions  
Hydrogen bond dynamics  
Vibrational spectral diffusion  
Escape dynamics of water  
Diffusion  
Orientational relaxation  
First principles simulation  
Time series analysis

## ABSTRACT

A theoretical study of vibrational spectral diffusion in aqueous NaBr solutions is presented by means of *ab initio* molecular dynamics simulations and time series analysis. The OD stretch frequencies of deuterated water hydrogen bonded to the bromide ions are found to be higher than those in the bulk which implies a somewhat weaker Br–water hydrogen bonds than those between water molecules. The dependence of OD stretch frequencies of hydration shell water on the length and angle of the associated ion–water hydrogen bonds is also investigated. The dynamics of frequency fluctuations of hydration shell and all water molecules are studied through calculations of hole dynamics and frequency time correlations. The roles of the dynamics of ion–water and water–water hydrogen bonds, escape dynamics of water from ion hydration shells and also that of other non-hydrogen-bonded dynamical modes in influencing the dynamics of vibrational spectral diffusion are discussed.

© 2012 Elsevier B.V. All rights reserved.

## 1. Introduction

Water molecules can form hydrogen bonds among themselves and also with many other ionic and polar solutes which play important roles in chemical processes in aqueous media. It is known that the hydrogen bond fluctuations have pronounced effects on the vibrational frequencies of water molecules, especially on the frequencies of stretch modes of water molecules. The temporal evolution of such frequency fluctuations, known as vibrational spectral diffusion, has been studied in many time dependent vibrational spectroscopic experiments to unearth the dynamics of hydrogen bond fluctuations in water and aqueous solutions [1–19]. There have also been a number of theoretical studies on vibrational spectral diffusion in aqueous media [20–29] and all these studies have provided much detailed information on the dynamical fluctuations in these systems at molecular level.

Regarding the dynamics of hydrogen bond fluctuations in aqueous ionic solutions, we note the recent experimental work of Refs. [16,17] where the dynamics of vibrational spectral diffusion in aqueous sodium bromide solutions was studied by means of time dependent vibrational spectroscopy. These studies reported a slow time scale of around 3–4 ps in addition to a shorter time scale of

less than a ps. The slow time scale was found to increase with salt concentration. For example, as the NaBr concentration was increased from 1.5 to 6.0 M, the slower time scale of vibrational spectral diffusion was found to increase from 2.6 to 4.8 ps [16]. We also note that this time scale of 3–4 ps as reported in recent experiments is different from an earlier study of the same solution where an order of magnitude slower time scale was reported [15]. On the theoretical side, the method of classical molecular dynamics simulation was employed to calculate the frequency fluctuations in aqueous NaI and NaBr solutions [23,25]. Very recently, theoretical studies were also conducted that went beyond the use of classical models and looked at the dynamics of spectral diffusion in water, supercritical water and aqueous solutions from first principles without using any empirical models [26–29]. In the latter studies, the method of *ab initio* molecular dynamics [30,31] was employed for the generation of dynamical trajectories and the fluctuating frequencies were calculated directly from the dynamical trajectories through a time series analysis [32]. The results were found to be in good agreement with experimental findings and, more importantly, no empirical potential needed to be used in these studies which seemed to be the key strength of these investigations. To the best of our knowledge, such first principles studies of vibrational spectral diffusion have not yet been carried out for aqueous NaBr solutions. The purpose of the present study is to make a contribution toward this end.

In the present study, we have investigated the distributions and dynamical fluctuations of vibrational frequencies of water

<sup>\*</sup> Corresponding author.

E-mail address: [amalen@iitk.ac.in](mailto:amalen@iitk.ac.in) (A. Chandra).

<sup>1</sup> Present address: Department of Chemistry, Indian Institute of Technology Hyderabad, Yaddumailaram 502205, Andhra Pradesh, India.

molecules in aqueous solutions containing sodium and bromide ions at two different concentrations by using the methods of first principles simulations and time series analysis. We have focused on the spectral behavior of both hydration shell and bulk water molecules and have investigated various structural and dynamical modes that can affect the distributions and dynamics of stretch frequencies of water molecules in the solutions. Specifically, we have looked at the frequency distributions of hydration shell water molecules that are hydrogen bonded to the bromide ions and also of other water molecules. The correlations between the frequencies of hydration shell water molecules with the ion–water hydrogen bond distances have also been explored. The dynamics of vibrational spectral diffusion is studied through calculations of hole dynamics and frequency correlation functions. The roles of hydrogen bond fluctuations, escape dynamics from hydration shells and also of other dynamical modes of non-hydrogen-bonded water molecules in the relaxation of vibrational spectral diffusion of water molecules in these solutions are discussed. The present results are also compared with the findings of recent experiments.

The rest of the paper is organized as follows. In Section 2, we have presented the details of first principles simulations and time series analysis. Our results of the distributions of vibrational frequencies of water molecules and frequency-structure correlations for the solution of a single bromide ion in water are presented in Section 3. In Section 4, we discuss the results of vibrational spectral diffusion in the two systems that are considered here with varying ion concentration. The relevance of various dynamical modes of water molecules to the dynamics of vibrational spectral diffusion is also discussed in this section. Finally, our conclusions are briefly summarized in Section 5.

## 2. Details of simulations and time series analysis

We have considered two aqueous solutions of varying concentration of  $\text{Br}^-$  ions. The relatively dilute ( $\sim 1.5$  M) solution consists of a  $\text{Br}^-$  ion immersed in a solvent of 31 water molecules and the concentrated solution ( $\sim 5$  M) contains 3  $\text{Na}^+$ , 3  $\text{Br}^-$  and 26 water molecules at room temperature. These two solutions will be referred to as Systems 1 and 2, respectively. The simulations were carried out using cubic boxes and the lengths of the boxes were determined from the experimental densities [33,34] of these two solutions. Periodic boundary conditions were applied in all directions. For System 1 without any counterion, the excess charge of the negative ion is assumed to be neutralized by a uniform background of opposite charge. The electronic structures of the extended systems were represented by the Kohn–Sham (KS) [35] formulation of density functional theory within the plane wave basis. For the core electrons, the Troullier–Martins [36] pseudopotentials were used and the plane wave expansions of the KS orbitals of the valence electrons were truncated at a kinetic energy cut-off of 80 Ry. We used a fictitious mass of  $\mu = 800$  a.u. for the electronic orbitals and the simulations were carried out using a time step of 5 a.u. We employed the BLYP [37] functional in the present calculations as was also done in many other *ab initio* simulations of aqueous ionic solutions [27,38–42]. The initial configurations of the two systems were generated using the classical molecular dynamics simulations [43] using empirical potentials [44,45]. During the *ab initio* simulations, each system was first equilibrated for approximately 10 ps in canonical ensemble. Subsequently, Systems 1 and 2 were run in microcanonical ensemble for 40 and 55 ps, respectively, for the calculations of various structural and dynamical properties.

The time dependent vibrational stretching frequencies of OD bonds were calculated from the simulation trajectories by using the so-called wavelet method of time series analysis. The details

of the wavelet analysis are available in Refs. [26,27,32,46]. In this method, a time dependent function  $f(t)$  is expressed in terms of basis functions which are constructed as translations and dilations of a mother wavelet  $\psi$

$$\psi_{a,b}(t) = a^{-\frac{1}{2}} \psi\left(\frac{t-b}{a}\right). \quad (1)$$

The coefficients of the wavelet expansion are given by the wavelet transform of  $f(t)$

$$L_{\psi}f(a, b) = a^{-\frac{1}{2}} \int_{-\infty}^{+\infty} f(t) \bar{\psi}\left(\frac{t-b}{a}\right) dt \quad (2)$$

for  $a > 0$  and  $b$  real. For the mother wavelet, we have used the so-called Morlet–Grossman wavelet [47]. The wavelet transform of Eq. (2) is a function of the variables  $a$  and  $b$ . As discussed in Ref.[32], the inverse of the scale factor  $a$  is proportional to the frequency and thus the wavelet transform at each  $b$  gives the frequency content of  $f(t)$  over a time window about  $b$ . Following our recent work on other aqueous systems [26–29,40], the time dependent function  $f(t)$  for a given OD bond is constructed to be a complex function with its real and imaginary parts corresponding to the instantaneous fluctuations in OD distance and the corresponding momentum along the OD bond at time  $t$ . The stretch frequency of this bond at a given time  $t = b$  is then determined from the scale  $a$  that maximizes the modulus of the corresponding wavelet transform at  $b$  and the process is then repeated for all the OD bonds that are present in the current simulation systems.

## 3. Distributions of vibrational frequencies of water near the bromide ion

In this Section, we discuss our results of the vibrational frequencies in the dilute solution of a single bromide ion in water. Thus, no counterion effects need to be considered for this system. Generally, the local environment of water molecules can be affected by presence of an ion which, in turn, can alter the vibrational frequencies of water molecules. For example, the stretch frequencies of water molecules in the solvation shell of the bromide ion are found to be different from those of the bulk molecules. In Fig. 1, we have

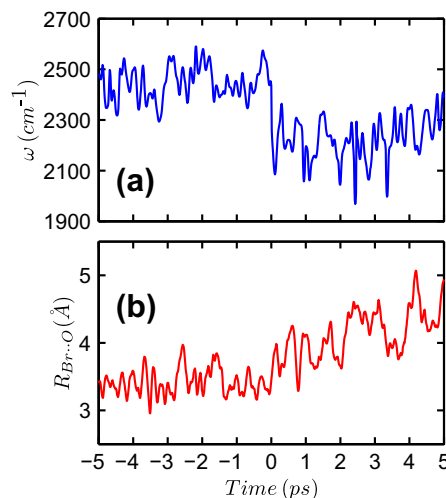


**Fig. 1.** The time dependence of the fluctuating frequency of an OD bond of water as it escapes from the solvation shell of  $\text{Br}^-$  to which it was hydrogen bonded initially. The time when the escape occurs i.e., when  $\text{Br} \cdots \text{O}$  distance exceeds 3.90 Å, is taken to be  $t = 0$  and the frequency and distance fluctuations are shown for ( $\pm 5$ ) ps before and after the escape event. (a) The time dependence of the frequency of the OD bond and (b) the corresponding  $\text{Br} \cdots \text{O}$  distance. The results of this figure and also of Figs. 2–4 are for the relatively dilute solution (System 1).

shown, how the instantaneous frequency of a tagged OD mode changes when it leaves the anionic solvation shell and diffuses into bulk. It is seen that there is a noticeable change in the average frequency of the OD bond and as the tagged water molecule leaves the hydration shell of  $\text{Br}^-$ , its OD stretch frequency decreases. In Fig. 2, we have shown the distribution of OD vibrational frequencies averaged over all the water molecules. In Fig. 2(a), we have shown the frequency distributions of OD bonds which are hydrogen bonded to the  $\text{Br}^-$  ion and also of those which are in the bulk water. The results are for the dilute solution (System 1). The corresponding frequency distributions for pure water [26] are also shown for comparison. The hydrogen bonds in the current systems are defined by employing the commonly used geometric criteria where a hydrogen bond between two water molecules or between a water molecule and ion exists if the following distance criteria are satisfied:  $R^{(XO)} < R_c^{(XO)}$  and  $R^{(XH)} < R_c^{(XH)}$ , where  $X$  denotes the oxygen of the first water molecule in the case of water–water hydrogen bonds and it denotes the  $\text{Br}^-$  ion in the case of anion–water hydrogen bonds. For our systems, the cut-off distance for  $R_c^{(XO)}$  is 3.35 Å when  $X$  is oxygen and it is 3.90 Å when  $X$  is a bromide ion. The value of  $R_c^{(XH)}$  is 2.45 Å when  $X$  is oxygen and 2.90 Å when  $X$  is a bromide ion. We note that these cut-off distances are essentially the positions of the first minimum of the oxygen–oxygen (bromide) and oxygen (bromide)–hydrogen radial distribution functions. In the inset of Fig. 2(a), we have shown the frequency distributions of the hydration shell and bulk OD groups, each normalized separately to 1.0 at the maximum in order to reveal more clearly the differences between these two distributions. In this figure, a blue shift in the stretching frequency of OD modes in the hydration shell water molecules is observed. The average frequencies of the anion hydration shell ( $\bar{\omega}_{\text{hyd}}$ ) and bulk ( $\bar{\omega}_b$ ) OD groups are found to be  $2400.2 \text{ cm}^{-1}$  and  $2369.6 \text{ cm}^{-1}$ , respectively. The present result of blue shift of the stretch frequency of water molecules in hydration shell of the bromide ion is in good agreement with the experimental results [16]. In spite of having an average frequency difference of  $\sim 30 \text{ cm}^{-1}$  between the bulk and hydration shell OD modes, the associated distributions are found to be rather wide

which means that the frequency shifts for individual escape events can be quite different from the average value. We note that an increase in hydrogen bond angle due to rotation generally leads to a weakening of the hydrogen bonds associated with an increase in  $\text{D}\cdots\text{O}$  and  $\text{D}\cdots\text{Br}$  distances and this, in turn, leads to an increase in the vibrational frequency of the covalent OD bonds. We have calculated the frequency distributions of hydrogen bonded OD modes for four different values of the hydrogen bond angle and the results are shown in Fig. 2(b). Expectedly, the distributions are found to shift to higher frequencies with increase of the hydrogen bond angle.

In order to get a better insight into the correlation between the frequencies of OD bonds in the hydration shell and the  $\text{D}\cdots\text{Br}$  hydrogen bond distances, we have performed a detailed analysis of the results that are averaged over all the OD groups pointing toward the  $\text{Br}^-$  ion in its hydration shell. In Fig. 3(a), we have shown the distributions of  $\text{D}\cdots\text{Br}$  distances for three fixed values of the OD frequency (within  $\pm 5 \text{ cm}^{-1}$ ). It is found that with increasing frequency, the corresponding distribution of  $\text{D}\cdots\text{O}$  distance is also shifted toward larger values. This correlation is more clearly shown in Fig. 3(b) through the contour plots of the conditional probability distribution of observing a particular frequency for a given hydrogen bond length. The rather wide distribution rules out the possibility of assigning a single instantaneous frequency to a given  $\text{D}\cdots\text{Br}$  distance. However, as shown by the dashed line, a correlation can be extracted on average where the frequency of an OD bond in the hydration shell decreases with a decrease in the associated  $\text{D}\cdots\text{Br}$  hydrogen bond distance. We note that similar correlations from first principles simulations were also found earlier for pure water and aqueous NaCl solutions [27]. In Fig. 4, we have shown the power spectrum of the velocity time correlation of the hydrogen atoms of the hydration shell water molecules. The power spectrum of the bulk water molecules is also shown here for comparison. We observe a blue shift of the stretch band and a red shift of the intermolecular band for the hydration shell water molecules compared to those of the bulk water. The results obtained from the power spectrum are in agreement with the results of Figs. 1–3 and also with the experimental results of infrared and low frequency Raman studies [48,49].

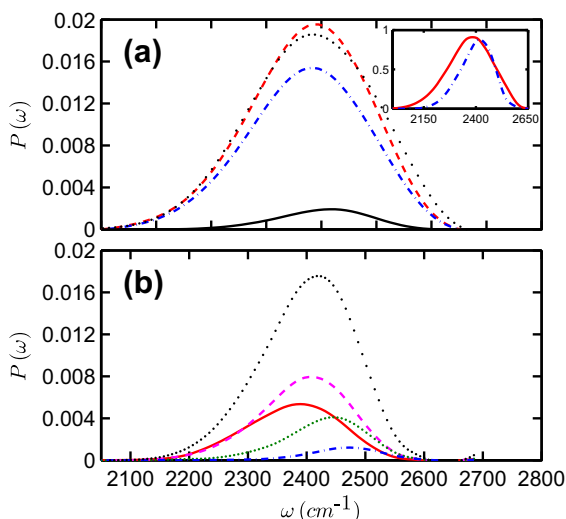


**Fig. 2.** (a) The distributions of OD stretch frequencies averaged over all OD modes (dashed), those in the bulk (dashed-dotted) and those in the  $\text{Br}^-$  hydration shell (solid). The dotted curve shows the corresponding distribution for pure water [26]. The inset shows the frequency distributions of bulk and hydration shell OD bonds each normalized to the maximum value of 1. (b) The frequency distributions for different values of the hydrogen bond angle  $\phi$ . The solid, dashed, dotted and dashed-dotted curves are for OD groups with hydrogen bond angles of  $5 \pm 5^\circ$ ,  $15 \pm 5^\circ$ ,  $25 \pm 5^\circ$  and  $35 \pm 5^\circ$ , respectively. The top dashed curve represents averages over all OD groups.

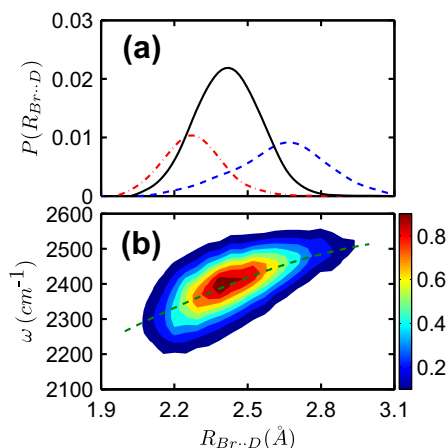


**Fig. 3.** (a) The distributions of the  $\text{Br}\cdots\text{D}$  distance for given values of the OD frequency. The solid, dashed-dotted and dashed curves are for the OD frequency  $\Delta\omega = 0 \pm 5 \text{ cm}^{-1}$ ,  $-100 \pm 5 \text{ cm}^{-1}$  and  $100 \pm 5 \text{ cm}^{-1}$ , respectively, where  $\Delta\omega$  represents the deviation from the average frequency. (b) The joint probability distribution of the OD frequency and  $\text{Br}\cdots\text{D}$  distance. The contour levels of different fractions of the maximum value are shown in different shades. The results are for water molecules in the  $\text{Br}^-$  hydration shell.

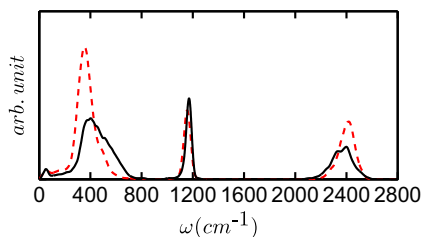


**Fig. 4.** The power spectrum of the velocity time correlation of deuterium atoms of heavy water in the  $\text{Br}^-$  hydration shell (dashed) and in the bulk region (solid) for System 1.

#### 4. Dynamics of vibrational spectral diffusion of water in presence of ions

In the hole burning technique of time dependent infrared spectroscopy, the time dependence of vibrational frequency fluctuations is investigated by exciting a band of OH or OD frequencies called the hole modes and subsequently probing their frequency variation with time. Upon excitation of the hole modes from the equilibrium distribution at the ground state, a nonequilibrium frequency distribution of the remaining water molecules is created. The characteristic time scales of the spectral shifts of the hole and remaining modes capture the dynamics of environmental fluctuations, especially the hydrogen bond fluctuations in the aqueous medium. It is assumed that a laser pump pulse having a Gaussian frequency profile creates a hole at  $t = 0$  in the ground state frequency distribution of the form [22,23,26,27]

$$P_h(\omega, 0) = P_{eq}(\omega) e^{-(\omega - \omega_p)^2 / 2\sigma^2}, \quad (3)$$

where  $\omega_p$  is the pulse center frequency and  $P_{eq}$  denotes the equilibrium frequency distribution of the OD modes of interest. Clearly, the initial distribution of the remaining OD frequencies  $P_r(\omega, 0)$ , i.e., the ones remaining in the ground state in experimental situations, is equal to  $P_{eq}(\omega) - P_h(\omega, 0)$ . We use a Gaussian pulse of full width ( $2\sigma$ ) equal to  $140 \text{ cm}^{-1}$  and calculate the time evolution of the non-equilibrium distributions  $P_r(\omega, t)$  and  $P_h(\omega, t)$  from a large set of system trajectories reflecting the initial distributions  $P_r(\omega, 0)$  and  $P_h(\omega, 0)$ , respectively. The average frequency of the hole modes at time  $t$  is then calculated from the following relation [22,23,26,27]

$$\bar{\omega}_h(t) = \frac{1}{N_h} \int d\omega \omega P_h(\omega, t), \quad (4)$$

where  $N_A = \int d\omega P_h(\omega, 0)$ . The average time dependent frequency of the remaining modes is calculated in a similar way by using the distribution of the remaining modes.

We first discuss the results for the relatively dilute solution of a single bromide ion in water. We choose a subset of the hydration shell OD modes for the hole dynamics calculations for this system. The average frequency shift of the hole modes of hydration shell water molecules has been studied by creating holes in two different frequency regions: one centered in the red side at  $\omega_p = \bar{\omega}_{hyd} - 100 \text{ cm}^{-1}$  and the other centered in the blue side at  $\omega_p = \bar{\omega}_{hyd} + 100 \text{ cm}^{-1}$  where  $\bar{\omega}_{hyd}$  is the average frequency of all the OD groups which are in the hydration shell of  $\text{Br}^-$  ion. Similar scheme is used here for the study of dynamics of the remaining OD modes inside the solvation shell. A Monte Carlo [43] type algorithm has been employed to create a hole in the red or blue region so that the distribution of Eq. (3) is satisfied.

In Fig. 5, we have shown the time evolution of average frequencies of the hole modes ( $\Delta\bar{\omega}_h$ ) for both blue and red excitations and the corresponding results for the remaining modes ( $\Delta\bar{\omega}_r$ ) are shown in Fig. 6. The frequency is expressed in terms of the shift ( $\Delta\omega$ ) from the equilibrium value averaged over all the modes.

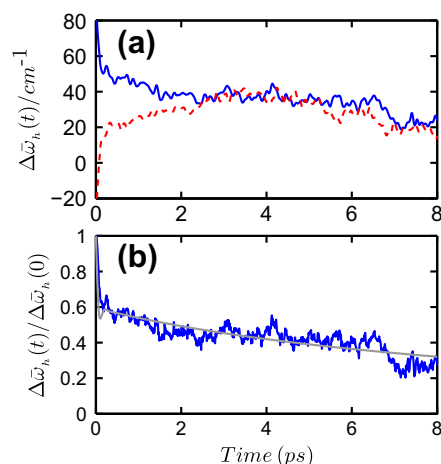


**Fig. 5.** The time dependence of the (a) average frequency shifts of the hole modes after they are selected (termed ‘excited’) in the blue and red sides of the hydration shell OD modes. The corresponding results for the blue excitation after normalization by the initial frequency shift are shown in (b). The solid and dashed curves corresponds to excitations in blue and red, respectively. The smooth grey solid curve in (b) represents the fit by a function of Eq. (5). The results are for the dilute solution (System 1). (For interpretation of the references to colour in this figure legend, the reader is referred to the web version of this article.)

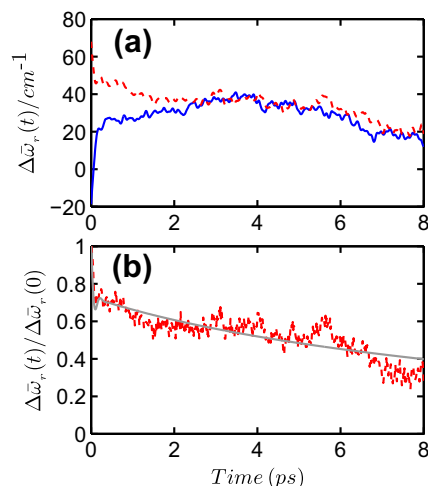


**Fig. 6.** The time dependence of the (a) average frequency shifts of the remaining modes after the hole was created in blue and in red sides of the hydration shell OD modes. The corresponding results for the red excitation after normalization by the initial frequency shift are shown in (b). As in the previous figure, the solid and dashed curves correspond to excitations in blue and red, respectively. The smooth grey solid curve in (b) represents the fit by a function of Eq. (5). The results are for the dilute solution (System 1). (For interpretation of the references to colour in this figure legend, the reader is referred to the web version of this article.)

We observe a fast decay and an oscillation at short times followed by slower decay extending to a few picoseconds. Since a bi- or tri-exponential fit does not reproduce the small oscillation or bump that is found at very short time, we used the following function including a damped oscillatory function to fit the calculated results of spectral diffusion [22,23,26–29]

$$f(t) = a_0 \cos(\omega_s t) e^{-\frac{t}{\tau_0}} + a_1 e^{-\frac{t}{\tau_1}} + (1 - a_0 - a_1) e^{-\frac{t}{\tau_2}} \quad (5)$$

and details of the relaxation times, frequency and the weights are include in Table 1. We have also performed a separate calculation of the power spectrum of the relative velocity of an initially hydrogen bonded  $\text{O} \cdots \text{Br}^-$  pair (results not shown). The calculated power spectrum reveals enhanced intensities at around  $40$  and  $140 \text{ cm}^{-1}$



**Table 1**

Spectral diffusion times with corresponding weights for the hydration shell OD modes of the dilute solution (System 1). The time constants (ps), frequency ( $\text{cm}^{-1}$ ) and the weights of time dependent frequency shifts of the hole and remaining modes for blue and red excitations of OD bonds in the  $\text{Br}^-$  hydration shell.

Quantity	Excitation	$\tau_0$	$\tau_1$	$\tau_2$	$\omega_s$	$a_0$	$a_1$
$\Delta\omega_h(t)$	Blue	0.056	3.52	19.32	127.4	0.40	0.13
$\Delta\omega_r(t)$	Red	0.072	3.12	18.0	132.484	0.27	0.12

due to intermolecular bending and stretching vibrations of the hydrogen bonded  $\text{Br}^-$ -water pairs. These bending and stretching modes of intermolecular vibrations can also influence the OD frequencies and hence can be responsible for the short-time oscillation of the hole dynamics.

In order to understand the origin of the slower time scales in the spectral diffusion, we looked at the relaxation of hydrogen bond fluctuations and escape dynamics of hydration shell water molecules. The dynamics of hydrogen bond fluctuations is studied by using the so-called population correlation function approach [50–58]. Specifically, we calculated the so-called continuous hydrogen bond correlation function that describes the probability that two water molecules (or an ion and a water), which were hydrogen bonded at time  $t = 0$ , remain continuously hydrogen bonded up to time  $t$  without ever breaking the hydrogen bond in the interim period. The integral of this correlation function gives the average lifetime of a hydrogen bond. Our calculated lifetimes of ion–water, water–water and all hydrogen bonds for both the systems are included in Table 2. The residence times of water molecules in the ion hydration shells are also calculated by following a similar population correlation function approach. Specifically, we calculated the probability that a water molecule, which was in the hydration shell of the ion at time  $t = 0$ , remains continuously in the same hydration shell up to time  $t$  subject to the allowance time  $t^*$ . The associated integrated relaxation time  $\tau_R$  gives the average residence time of water molecule in the hydration shell of the ion. We calculated the residence time  $\tau_R$  by explicit integration of the residence probability function from simulations until 24 ps and by calculating the integral for the tail part from fitted exponential functions. For our calculation of residence dynamics, we have taken the allowance time 2 ps [27,59] for the continuous residence function and found a value of 20.4 ps for the residence time of water molecules in the  $\text{Br}^-$  solvation shell for the dilute solution. The above results for the hydration shell water appear to suggest that the two slower relaxation times of the spectral diffusion of water molecules in  $\text{Br}^-$  hydration shell originate from the hydrogen bond dynamics of anion–water pairs and the escape dynamics of water molecules from the anion hydration shell.

Till now, we have considered the dynamical response of only the hydration shell water molecules. It would also be instructive to look at the spectral diffusion of all the OD modes of the solutions since the spectral response in an experimental situation includes contributions from both the hydration shell and bulk water molecules. The results of such calculations are presented in Figs. 7, 8 and

**Table 2**

The average lifetimes of bromide ion–water and all hydrogen bonds (HBs) of the relatively dilute (System 1) and concentrated (System 2) solutions. Results are also included for the residence times of water in the ion hydration shell. All time constants are expressed in ps.

Quantity	System	Ion–water HBs	All HBs
$\tau_{HB}$	1	1.75	3.2
$\tau_R$	1	18.0	–
$\tau_{HB}$	2	2.2	2.5
$\tau_R$	2	20.3	–

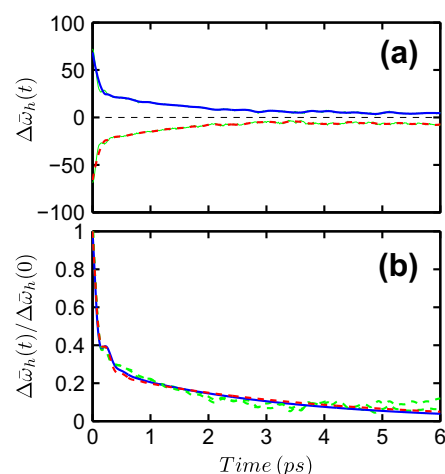


**Fig. 7.** The dynamics of the (a) average frequency shifts of the hole modes when all OD modes are considered in the calculations. The corresponding results after normalization by the initial frequency shifts are shown in (b). As before, the solid and dashed curves correspond to excitations in blue and red, respectively. The solid and dashed curves in (b) represent the fits by a function of Eq. (5). The results are for the dilute solution (System 1). (For interpretation of the references to colour in this figure legend, the reader is referred to the web version of this article.)

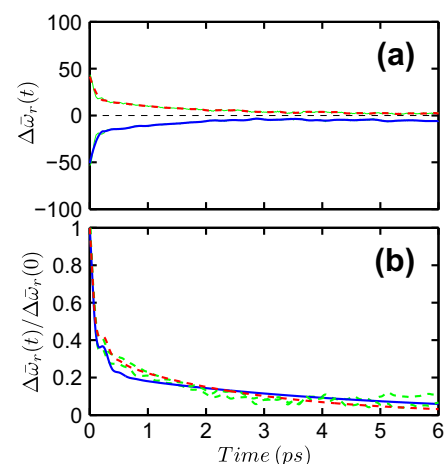


**Fig. 8.** The dynamics of the (a) average frequency shifts of the remaining modes when all OD modes are considered in the calculations. The corresponding results after normalization by the initial frequency shifts are shown in (b). As before, the solid and dashed curves correspond to excitations in blue and red, respectively. The solid and dashed curves in (b) represent the fits by a function of Eq. (5). The results are for the dilute solution (System 1). (For interpretation of the references to colour in this figure legend, the reader is referred to the web version of this article.)

**Table 3**

Spectral diffusion times with corresponding weights for all OD modes of the relatively dilute (System 1) and concentrated (System 2) solutions. The units of different quantities are as in Table 1.

Quantity	Systems	Excitation	$\tau_0$	$\tau_1$	$\tau_2$	$\omega_s$	$a_0$	$a_1$
$C_\omega(t)$	1	–	0.114	0.15	2.9	112.0	0.22	0.43
$\Delta\omega_h(t)$	1	Blue	0.12	0.17	3.0	112.10	0.27	0.45
$\Delta\omega_r(t)$	1	Blue	0.13	0.17	4.6	113.83	0.23	0.55
$\Delta\omega_h(t)$	1	Red	0.16	0.15	3.6	117.20	0.16	0.58
$\Delta\omega_r(t)$	1	Red	0.12	0.16	2.6	112.10	0.22	0.45
$C_\omega(t)$	2	–	0.08	0.15	4.3	109.35	0.28	0.45
$\Delta\omega_h(t)$	2	Blue	0.18	0.12	3.9	129.94	0.10	0.65
$\Delta\omega_r(t)$	2	Blue	0.18	0.12	5.3	129.43	0.10	0.62
$\Delta\omega_h(t)$	2	Red	0.21	0.12	5.0	127.60	0.06	0.63
$\Delta\omega_r(t)$	2	Red	0.22	0.11	3.5	130.45	0.055	0.67

**Table 3.** In general, it is found that the decay is faster as compared to the one found for the hydration shell OD modes only in the dilute solution. In particular, the slowest component corresponding to the escape dynamics of water from ion solvation shell appears to be absent. In addition to the time dependent spectral shifts, another dynamical object which is looked at in the studies of vibrational spectral diffusion is the frequency time correlation function defined as

$$C_{\omega}(t) = \frac{\langle \delta\omega(t)\delta\omega(0) \rangle}{\langle \delta\omega(0)^2 \rangle}, \quad (6)$$

where  $\delta\omega(t)$  is the fluctuation from the average frequency of an OD mode at time  $t$ . The average of Eq. (6) is over the initial time and over all the OD groups of the system.

The results of the frequency time correlation are shown in Fig. 9. At this stage, we also like to discuss the results for the concentrated solution that contains both sodium and bromide ions. Hence, in Fig. 9, in addition to the results of the dilute solution, we have also included the results of the frequency correlation of the concentrated solution (System 2) averaged over all OD modes. Overall, the decay pattern of the frequency correlations is found to be similar to those of the frequency shifts of hole dynamics calculations shown in Figs. 7 and 8. The results for the hole and remaining modes for the concentrated solution (System 2) averaged over all the OD modes are shown in Figs. 10 and 11. There is a fast decay and an oscillation at short times, followed by a slower decay extending to few picoseconds. A fit of the type of Eq. (5) produces a fast time constants around 150 fs and a slower time constant around 3 ps. The details of these time constants are included in Table 3. The shorter time scale corresponds to the frequency modulation due to the dynamics of intact hydrogen bonds while the longer time constant is attributed to the lifetimes of hydrogen bonds, now averaged over both ion–water and water–water pairs.

It is seen that, for both dilute (System 1) and the concentrated (System 2) solutions, no long time decay with time constant of  $\sim 20$  ps is found either in the frequency correlation or in the spectral shifts calculated for all the OD modes. This slowest time scale originated from the escape dynamics of water molecules from the ion-hydration shells and it was found to show up in the long-time decay of the spectral diffusion in System 1 when only the hydration shell OD modes were considered in the calculations. This slow time scale is found to be absent when the calculations were done with all OD modes which is likely due to the very small weight of the hydration water to the overall spectral response of all the OD modes at low concentration. This slow component is found to be absent for the concentrated solution also even though the fraction of such water molecules in the anion hydration shells is now

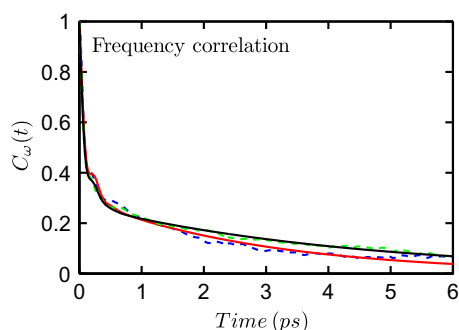


**Fig. 9.** The time correlation functions of OD fluctuating frequencies averaged over all the water molecules of the dilute (System 1) and concentrated (System 2) solutions. The lower and upper dashed curves correspond to the simulation results for Systems 1 and 2, respectively. The solid curves represent the fits by a function as given by Eq. (5).

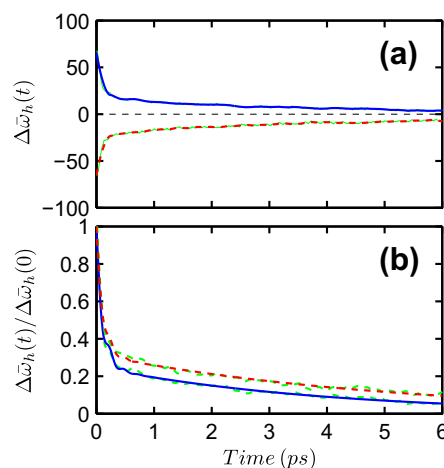


**Fig. 10.** The time dependence of the (a) average frequency shifts of the hole modes when all OD modes are considered in the calculations. The corresponding results after normalization by the initial frequency shifts are shown in (b). As before, the solid and dashed curves correspond to excitations in blue and red, respectively. The solid and dashed curves in (b) represent the fits by a function of Eq. (5). The results are for the concentrated solutions (System 2). (For interpretation of the references to colour in this figure legend, the reader is referred to the web version of this article.)

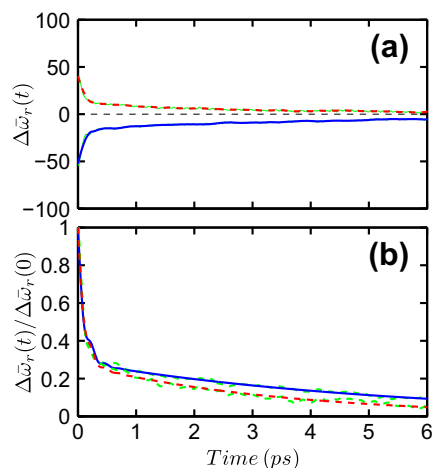


**Fig. 11.** The time dependence of the (a) average frequency shifts of the remaining modes when all OD modes are considered in the calculations. The corresponding results after normalization by the initial frequency shifts are shown in (b). As before, the solid and dashed curves correspond to excitations in the blue and red, respectively. The solid and dashed curves in (b) represent the fits by a function of Eq. (5). The results are for the concentrated solution (System 2).

significant. The higher ion concentration ensures that whenever a water molecule leaves an ion-hydration shell, it quickly enters the hydration shell of another ion. In addition,  $\text{Na}^+$  and  $\text{Br}^-$  ions reduce the water–water correlations resulting in an increase in the frequencies of even those OD modes which are not in the solvation shells. For example, the average OD frequencies of water molecules inside the hydration shells of bromide and sodium ions and outside of them are found to be 2404, 2395 and 2393  $\text{cm}^{-1}$ , respectively, for the concentrated solution. Thus, the escape of a water molecule from an ion hydration shell takes place without any significant changes in its stretch frequency as can be seen in Fig. 12. Therefore, a clear distinction between the hydration shell and bulk water in terms of their stretch frequencies does not seem to exist at high ion concentration and now the slower component of the overall spectral diffusion is simply influenced, in part, by the hydrogen

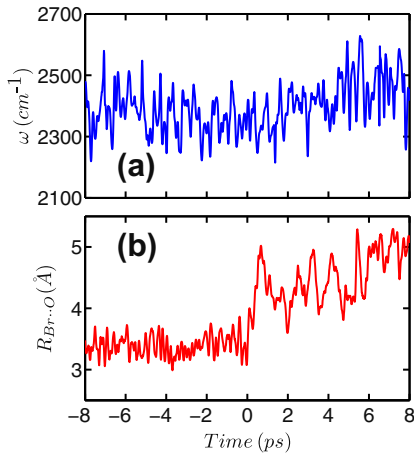


**Fig. 12.** The time dependence of the fluctuating frequency of an OD bond of water as it leaves the solvation shell of a  $\text{Br}^-$  ion in the concentrated solution (System 2). The time instant of the escape i.e., when  $\text{Br} \cdots \text{O}$  distance exceeds  $3.90 \text{ \AA}$ , is taken to be  $t = 0$  and the frequency and distance fluctuations are shown for  $(\pm 8)$  ps before and after the escape event. (a) The time dependence of the frequency of the OD bond and (b) the corresponding  $\text{Br} \cdots \text{O}$  distance.

bond dynamics of ion-water and water-water pairs. We note that similar results of not so different vibrational frequencies of water molecules inside and outside the anion hydration shells were also found earlier for concentrated aqueous solution of sodium chloride [27].

The present result of an increase of the vibrational spectral diffusion time with increase of ion concentration is in agreement with recent experiments [16]. We note in this context, however, that the hydrogen bond lifetimes are found to follow the following trend with increase of ion concentration: (a) Bromide ion–water hydrogen bond lifetime increases, (b) water–water hydrogen bond lifetime decreases and (c) average lifetime of all hydrogen bonds, i.e. anion–water plus water–water, decreases with increase of ion concentration. Hence it appears that the hydrogen bond breaking dynamics, although it plays an important role in spectral diffusion, is not the only factor that influences spectral diffusion. In an attempt to understand other dynamical processes that might influence the spectral diffusion, we calculated the diffusion and orientational relaxation of ions and water molecules for both concentrations. The diffusion coefficients ( $D$ ) are obtained by integrating the normalized velocity-velocity autocorrelation functions of water molecules or ions

$$D = \frac{k_B T}{m} \int_0^\infty C_v(t) dt, \quad (7)$$

where  $k_B$  is the Boltzmann constant,  $T$  is the temperature and  $m$  is the mass of a water molecule or an ion and  $C_v(t)$  is the normalized velocity-velocity autocorrelation function

$$C_v(t) = \frac{\langle v(t) v(0) \rangle}{\langle v(0)^2 \rangle}, \quad (8)$$

The orientational relaxation time  $\tau_l^\alpha$  is obtained as the time integral of the orientational correlation function

$$C_l^\alpha(t) = \frac{\langle P_l[e^\alpha(t) \cdot e^\alpha(0)] \rangle}{\langle P_l[e^\alpha(0) \cdot e^\alpha(0)] \rangle}, \quad (9)$$

$$\tau_l^\alpha = \int_0^\infty C_l^\alpha(t) dt, \quad (10)$$

where  $P_l$  is the Legendre polynomial of rank  $l$  and  $e^\alpha$  is the unit vector which points along the  $\alpha$ th axis in the water molecular frame.

**Table 4**

The diffusion coefficients (in  $10^{-5} \text{ cm}^2 \text{ s}^{-1}$ ) and orientational relaxation times (in ps) of water molecules in the vicinity of bromide ions and in the bulk.

Quantity	System	Hydration shell	Bulk
$D$	1	0.60	0.64
$D$	2	0.22	0.40
$\tau_2^{OH}$	1	5.6	5.0
$\tau_2^{OH}$	2	9.6	6.0

We have calculated  $\tau_l^\alpha$  for  $l = 2$  and for the O–H vectors. These orientational relaxation times were obtained by explicit integration of  $C_l^\alpha(t)$  from simulations until 30 ps and by calculating the integral for the tail from the fitted exponential functions. For water molecules, we have calculated the diffusion coefficients and orientational relaxation times separately for hydration shell and bulk water molecules and the results are shown in Table 4. This Table also includes the diffusion coefficients of ions in the solutions. A slowing down of the rate of these single-particle dynamics is observed with increase of ion concentration. We further calculated the potential of mean force of bromide ion–water and water–water pairs from the logarithms of the corresponding ion–oxygen and oxygen–oxygen radial distribution functions and the results are shown in Fig. 13. An analysis of the potentials of mean force reveals that the hydrogen bond lifetime of water–water pairs primarily decreases due to a slight decrease of the well depth and an enhanced population of water molecules near the dividing surface.

Although the hydrogen bond fluctuations play important roles in changing the frequencies, the electric field of an ion can continue to influence the OD vibrations even after the ion–water hydrogen bond is broken as per the adopted geometric definition of such a bond or when the water is in the vicinity of cations which do not form any hydrogen bonds. In such cases, diffusion and orientational relaxation would also play a role in addition to hydrogen bond lifetimes as these motion can also alter the electric field fluctuations on the OD bonds, hence their frequencies. The importance of non-hydrogen bonded ion–water pairs can also be gauged from the fact that while the coordination number of a bromide ion is around 7 at both concentrations, only 35% out of them are found to be hydrogen bonded. The remaining water molecules stay in the hydration shell more through ion–dipole interactions rather than hydrogen bonding interactions. Such ion–dipole interactions can also be rather strong for water molecules in the cation hydra-

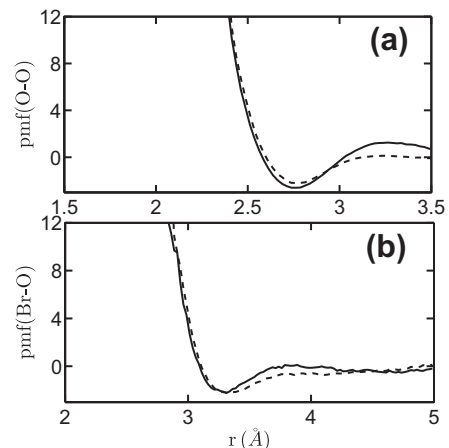


**Fig. 13.** (a) The (a) oxygen–oxygen and (b) bromide ion–oxygen potentials of mean force (in units of  $k_B T$ ) in the dilute (System 1) and concentrated (System 2) sodium bromide solutions are shown. The solid curves are for System 1 and the dashed curves are for System 2.

tion shells. However, for cations, the oxygen atoms of water molecules point toward the cation and the hydrogens point outward. Since the hydrogens of such water molecules in the cation hydration shells can form hydrogen bonds with other water molecules or anions, the frequencies of OD bonds of those water molecules are expected to be very similar to those of bulk water or of the anion hydration shells. This is indeed the case as can be seen from the values of average OD frequencies in cation and anion hydration shells given in the earlier part of this Section. The dynamical changes of such ion–dipole interactions which are influenced by slower diffusion and orientational relaxation at higher concentration can also alter the vibrational frequencies of OD bonds. The contributions from slower diffusion and orientational relaxation of surrounding ions and water molecules even when the OD mode of interest is not hydrogen bonded qualitatively explain (i) why the spectral diffusion of hydration shell water molecules is slower than bromide ion–water hydrogen bond lifetime for the dilute solution, and also (ii) why the spectral diffusion time of aqueous NaBr solution increases with increase of ion concentration which is in agreement with experimental observations [16].

## 5. Summary and conclusions

In this work, we have investigated the vibrational frequency distributions and dynamics of spectral diffusion of deuterated water molecules in aqueous ionic solutions containing bromide and sodium ions from first principles without using any predefined empirical interaction potentials. Two different concentrations of the ions have been considered in the present study. Our calculations are based on *ab initio* molecular dynamics simulations within density functional theory for trajectory generation and the wavelet method of time series analysis for calculations of fluctuating frequencies. It is found that the stretch frequencies of OD bonds that are hydrogen bonded to the bromide ions are higher than those which are hydrogen bonded to other water molecules implying that the bromide ion–water hydrogen bonds are somewhat weaker than those between water molecules. In general, the stretch frequencies of hydration shell OD modes are found to increase with increase of the length of the associated ion–water hydrogen bonds or with increase of the corresponding hydrogen bond angle. Significant dispersions are also found in the frequency distributions which mean the assignment of a definite OD stretch frequency to a given instantaneous hydrogen bond length or angle is not possible. However, on average, the stretch frequencies of OD modes are found to increase with increase of hydrogen bond length as was also found earlier for pure water and ionic solutions in both classical and *ab initio* simulation studies [22–27]. In the present study, it is also found that a significant fraction of water molecules in the  $\text{Br}^-$  hydration shell stay without being hydrogen bonded. Thus, for the hydration shell water of  $\text{Br}^-$  ions, non-hydrogen-bonded ion–dipole interactions are also found to play a significant role in addition to hydrogen bonded interactions and the dynamical fluctuations of such non-hydrogen-bonded interactions are found to influence the time scales of spectral diffusion of water molecules in these solutions.

The vibrational spectral diffusion of hydration shell and all water molecules are investigated through calculations of hole dynamics and frequency time correlations. When the vibrational spectral diffusion is studied exclusively for the hydration shell water of the relatively dilute solution (System 1), the dynamics revealed three time scales: a fast relaxation of  $\sim 200$  fs; a slower relaxation of  $\sim 3$  ps and another slower time constant of  $\sim 20$  ps. However, when the vibrational spectral diffusion is calculated for all the OD modes, only two time scales of  $\sim 150$  fs and  $\sim 2.9$  ps are found without the slowest component of  $\sim 20$  ps. This is likely

due to the smaller weight that hydration shell water makes to overall spectral diffusion of all the molecules so that the slowest component, which originates from the escape of hydration shell water, is not noticeable in the total response. This slow time constant of  $\sim 20$  ps is also not seen in the spectral diffusion of all the OD modes in the concentrated solution as no significant frequency changes were found on escape of a water molecule from an anionic hydration shell to outside of it. The fast time constant corresponds to the dynamics of intact ion–water hydrogen bonds. The intermediate time scale of  $\sim 3$  ps does not correspond fully to the hydrogen bond lifetime because the anion–water hydrogen bonds are weak and have a faster lifetime than this value. Also, the average lifetime of all hydrogen bonds in the solutions decreases with increasing ion concentration which is opposite to the trend for the spectral diffusion time when all modes are considered in the calculations. Clearly, the vibrational spectral diffusion in the present solutions is influenced by other dynamical channels in addition to the hydrogen bond fluctuations. This is also supported by the fact that a significant number of water molecules in the  $\text{Br}^-$  hydration shells are not hydrogen bonded. The water molecules in the cation hydration shells are also held through ion–dipole interactions. These non-hydrogen-bonded molecules stay in the ion hydration shell more due to attractive ion–dipole interactions and the dynamical fluctuations of such interactions as governed by slower diffusion and orientational relaxation of ions and water molecules also likely influence the frequency fluctuations, hence the dynamics of vibrational spectral diffusion in the present ionic solutions. We also note in this context that due to limited length of the dynamical trajectories (40–55 ps) of our first principles simulations, the decay of spectral shifts and frequency correlations could be meaningfully investigated for about 6–8 ps. A recent classical molecular dynamics based study on vibrational spectral diffusion in aqueous NaBr solutions, which could look at the spectral diffusion for a much longer time by generating trajectories of 2.5 ns length, reported the presence of additional slower time scales at longer times [25]. It would be interesting to extend the present first principles study to such longer simulation times and explore the spectral dynamics at times beyond what could be achieved in the current study.

## Acknowledgement

We gratefully acknowledge financial supports from the Department of Science and Technology (DST) and the Council of Scientific and Industrial Research (CSIR), Government of India.

## References

- [1] J.B. Asbury, T. Steinel, C. Stromberg, S.A. Corcelli, C.P. Lawrence, J.L. Skinner, M.D. Fayer, *J. Phys. Chem. A* 108 (2004) 1107.
- [2] H.J. Bakker, J.L. Skinner, *Chem. Rev.* 110 (2010) 1498; H.J. Bakker, *Chem. Rev.* 108 (2008) 1456.
- [3] H.J. Bakker, M.F. Kropman, A.W. Omta, S. Woutersen, *Phys. Scr.* 69 (2004) C14.
- [4] E.T.J. Nibbering, T. Elsaesser, *Chem. Rev.* 104 (2004) 1887.
- [5] R. Laenen, C. Rauscher, A. Laubereau, *Phys. Rev. Lett.* 80 (1998) 2622; R. Laenen, K. Simeonidis, A. Laubereau, *J. Phys. Chem. B* 106 (2002) 408.
- [6] S. Woutersen, U. Emmerichs, H.J. Bakker, *Science* 278 (1997) 658; S. Woutersen, H.J. Bakker, *Phys. Rev. Lett.* 83 (1999) 2077.
- [7] G.M. Gale, G. Gallot, F. Hache, N. Lascoux, S. Bratos, *Phys. Rev. Lett.* 82 (1999) 1068; S. Bratos, G.M. Gale, G. Gallot, F. Hache, N. Lascoux, J.-C. Leickman, *Phys. Rev. E* 61 (2001) 5211.
- [8] Z. Wang, A. Pakoulev, Y. Pang, D.D. Dlott, *Chem. Phys. Lett.* 378 (2003) 281; A. Pakoulev, Z. Wang, Y. Pang, D.D. Dlott, *Chem. Phys. Lett.* 371 (2003) 594.
- [9] T. Steinel, J.B. Asbury, S.A. Corcelli, C.P. Lawrence, J.L. Skinner, M.D. Fayer, *Chem. Phys. Lett.* 386 (2004) 295; J.B. Asbury, T. Steinel, K. Kwak, S.A. Corcelli, C.P. Lawrence, J.L. Skinner, M.D. Fayer, *J. Chem. Phys.* 121 (2004) 12431.
- [10] C.J. Fecko, J.D. Eaves, J.J. Loparo, A. Tokmakoff, P.L. Geissler, *Science* 301 (2003) 1698;



- J.D. Eaves, J.J. Loparo, C.J. Fecko, S.T. Roberts, A. Tokmakoff, P.L. Geissler, *Proc. Natl. Acad. Sci. U.S.A* 102 (2005) 13019.
- [11] C.J. Fecko, J.J. Loparo, S.T. Roberts, A. Tokmakoff, *J. Chem. Phys.* 122 (2005) 054506;
- S.T. Roberts, J.J. Loparo, A. Tokmakoff, *J. Chem. Phys.* 125 (2006) 084502.
- [12] J.J. Loparo, S.T. Roberts, A. Tokmakoff, *J. Chem. Phys.* 125 (2006) 194521.
- [13] J. Stenger, D. Madsen, P. Hamm, E.T.J. Nibbering, T. Elsaesser, *J. Phys. Chem. A* 106 (2002) 2341;
- M.L. Cowan, B.D. Bruner, N. Huse, J.R. Dwyer, B. Chugh, E.T.J. Nibbering, R.J.D. Miller, *Nature (London)* 434 (2005) 199.
- [14] A. Omta, M.F. Kropman, S. Wouterson, H.J. Bakker, *Science* 301 (2003) 347.
- [15] M.F. Kropman, H.J. Bakker, *Science* 291 (2001) 2118;
- M.F. Kropman, H.J. Bakker, *J. Chem. Phys.* 115 (2001) 8942.
- [16] S. Park, M.D. Fayer, *Proc. Natl. Acad. Sci. USA* 104 (2007) 16731.
- [17] R.L.A. Timmer, H.J. Bakker, *J. Phys. Chem. A* 113 (2009) 6104.
- [18] S. Park, M. Odelius, K.J. Gaffney, *J. Phys. Chem. B* 113 (2009) 7825.
- [19] J. Minbiao, M. Odelius, K.J. Gaffney, *Science* 328 (2010) 1003.
- [20] J.L. Skinner, B.M. Auer, Y.S. Lin, *Adv. Chem. Phys.* 142 (2009) 59.
- [21] J.L. Skinner, *Science* 328 (2010) 985.
- [22] R. Rey, K.B. Moller, J.T. Hynes, *J. Phys. Chem. A* 106 (2002) 11993;
- K.B. Moller, R. Rey, J.T. Hynes, *J. Phys. Chem. A* 108 (2004) 1275.
- [23] B. Nigro, S. Re, D. Laage, R. Rey, J.T. Hynes, *J. Phys. Chem. A* 110 (2006) 11237.
- [24] C.P. Lawrence, J.L. Skinner, *Chem. Phys. Lett.* 369 (2003) 472;
- C.P. Lawrence, J.L. Skinner, *J. Chem. Phys.* 117 (2003) 8847;;
- C.P. Lawrence, J.L. Skinner, *J. Chem. Phys.* 118 (2003) 264.
- [25] Y.-S. Lin, B.M. Auer, J.L. Skinner, *J. Chem. Phys.* 131 (2009) 144511.
- [26] B.S. Mallik, A. Semparathi, A. Chandra, *J. Phys. Chem. A* 112 (2008) 5104;
- B.S. Mallik, A. Chandra, *J. Phys. Chem. A* 112 (2008) 13518.
- [27] B.S. Mallik, A. Semparathi, A. Chandra, *J. Chem. Phys.* 129 (2008) 194512.
- [28] R. Gupta, A. Chandra, *J. Mol. Liq.* 165 (2012) 1.
- [29] D. Chakraborty, A. Chandra, *J. Chem. Phys.* 135 (2011) 114510;
- D. Chakraborty, A. Chandra, *Chem. Phys.* 392 (2012) 96.
- [30] R. Car, M. Parrinello, *Phys. Rev. Lett.* 55 (1985) 2471.
- [31] D. Marx, J. Hutter, *Ab Initio Molecular Dynamics: Basic Theory and Advanced Methods*, Cambridge University Press, Cambridge, 2009.
- [32] L.V. Vela-Arevalo, S. Wiggins, *Int. J. Bifurcation Chaos Appl. Sci. Eng.* 11 (2001) 1359.
- [33] D.R. Lide (Ed.), *Handbook of Chemistry and Physics*, vol. 87, CRC, Taylor & Francis, Boca Raton, FL; London, 2006.
- [34] M. Laliberete, W.E. Cooper, *J. Chem. Eng. Data* 49 (2004) 1141.
- [35] W. Kohn, L.J. Sham, *Phys. Rev.* 140 (1965) A1133.
- [36] N. Troullier, J.L. Martins, *Phys. Rev. B* 43 (1991) 1993.
- [37] A.D. Becke, *Phys. Rev. A* 38 (1998) 3098;
- C. Lee, W. Yang, R.G. Parr, *Phys. Rev. B* 37 (1988) 785.
- [38] S. Rauegi, M.L. Klein, *J. Am. Chem. Soc.* 123 (2001) 9484;
- S. Rauegi, M.L. Klein, *J. Chem. Phys.* 116 (2002) 196.
- [39] J.M. Heuft, E.J. Meijer, *J. Chem. Phys.* 119 (2003) 11788;
- J.M. Heuft, E.J. Meijer, *J. Chem. Phys.* 123 (2005) 094506.
- [40] Bhabani S. Mallik, A. Chandra, *Chem. Phys.* 387 (2011) 48.
- [41] M.M. Naor, K.V. Nostrand, C. Dellago, *Chem. Phys. Lett.* 369 (2003) 159.
- [42] D.J. Tobias, P. Jungwirth, M. Parrinello, *J. Chem. Phys.* 114 (2001) 7036.
- [43] M.P. Allen, D.J. Tildesley, *Computer Simulation of Liquids*, Oxford, New York, 1987.
- [44] H.J.C. Berendsen, J.R. Grigera, T.P. Straatsma, *J. Phys. Chem.* 91 (1987) 6269.
- [45] L.X. Dang, *Chem. Phys. Lett.* 200 (1992) 21;
- L.X. Dang, B.C. Garrett, *J. Chem. Phys.* 99 (1993) 2972.
- [46] A. Semparathi, S. Keshavamurthy, *Phys. Chem. Chem. Phys.* 5 (2003) 5051.
- [47] R. Carmona, W. Hwang, B. Torresani, *Practical Time-Frequency Analysis: Gabor and Wavelet Transforms with an Implementation*, Academic, New York, 1998.
- [48] J.J. Max, C. Chapados, *J. Chem. Phys.* 115 (2001) 2664.
- [49] Y. Wang, Y. Tominaga, *J. Chem. Phys.* 101 (1994) 3453;
- K. Mizoguchi, T. Ujike, Y. Tominaga, *J. Chem. Phys.* 109 (1998) 1867;
- Y. Amo, Y. Tominaga, *Phys. Rev. E* 58 (1998) 7553.
- [50] D. Rapaport, *Mol. Phys.* 50 (1983) 1151.
- [51] A. Luzar, D. Chandler, *Nature (London)* 53 (1996) 379;
- A. Luzar, *J. Chem. Phys.* 113 (2000) 10663.
- [52] A. Chandra, *Phys. Rev. Lett.* 85 (2000) 768;
- S. Chowdhuri, A. Chandra, *J. Chem. Phys.* 115 (2001) 3732.
- [53] S. Balasubramanian, S. Pal, B. Bagchi, *Phys. Rev. Lett.* 89 (2002) 115505.
- [54] H. Xu, H.A. Stern, *J. Phys. Chem. B* 105 (2001) 11929;
- H. Xu, H.A. Stern, B.J. Berne, *J. Phys. Chem. B* 106 (2002) 2054.
- [55] E. Guardia, D. Laria, J. Marti, *J. Phys. Chem. B* 110 (2006) 6332;;
- E. Guardia, J. Marti, L. Garcia-Tarres, D. Laria, *J. Mol. Liq.* 117 (2005) 63.
- [56] S.K. Pattanayak, S. Chowdhuri, *J. Phys. Chem. B* 115 (2011) 13241.
- [57] J. Chanda, S. Bandyppadhyay, *J. Chem. Theory. Comput.* 1 (2005) 963;
- J. Chanda, S. Bandyppadhyay, *J. Phys. Chem. B* 110 (2006) 23482.
- [58] S. Paul, G.N. Patey, *J. Am. Chem. Soc.* 129 (2007) 4476;
- R. Sarma, S. Paul, *J. Chem. Phys.* 136 (2012) 114510.
- [59] R.W. Impey, P.A. Madden, I.R. McDonald, *J. Phys. Chem.* 87 (1983) 5071.